

High-redshift QSOs in the GOODS

S.Cristiani¹, D.M.Alexander^{2,10}, F.Bauer², W.N.Brandt², E.T.Chatzichristou³, F.Fontanot⁴, A.Grazian⁵, A.Koekemoer⁶, R.A.Lucas⁶, J.Mao¹¹, P.Monaco⁴, M.Nonino¹, P.Padovani^{6,9}, D.Stern⁷, P.Tozzi¹, E.Treister³, C.M.Urry³, and E.Vanzella⁸

¹ INAF-Osservatorio Astronomico, Via Tiepolo 11, I-34131 Trieste, Italy

² Department of Astronomy and Astrophysics, Pennsylvania State University, 525 Davey Lab, University Park, PA 16802

³ Department of Astronomy, Yale University, PO Box 208101, New Haven, CT06520

⁴ Dipartimento di Astronomia dell'Università, Via Tiepolo 11, I-34131 Trieste, Italy

⁵ INAF-Osservatorio Astronomico di Roma, via Frascati 33, I-00040 Monteporzio, Italy

⁶ Space Telescope Science Institute, 3700 San Martin Dr., Baltimore, MD 21218

⁷ Jet Propulsion Laboratory, California Institute of Technology, Mail Stop 169-506, Pasadena, CA 91109

⁸ European Southern Observatory, K.Schwarzschild-Straße 2, D-85748 Garching, Germany

⁹ ESA Space Telescope Division

¹⁰ Institute of Astronomy, Madingley Road, Cambridge, CB3 0HA, UK

¹¹ SISSA, via Beirut 4, I-34014 Trieste, Italy

1 Introduction

QSOs are intrinsically luminous and therefore can be seen rather easily at large distances; but they are rare, and finding them requires surveys over large areas. As a consequence, at present, the number density of QSOs at high redshift is not well known. Recently, the Sloan Digital Sky Survey (SDSS) has produced a breakthrough, discovering QSOs up to $z = 6.43$ [8] and building a sample of six QSOs with $z > 5.7$. The SDSS, however, has provided information only about very luminous QSOs ($M_{1450} \lesssim -26.5$), leaving unconstrained the faint end of the high- z QSO Luminosity Function (LF), which is particularly important to understand the interplay between the formation of galaxies and super-massive black holes (SMBH) and to measure the QSO contribution to the UV ionizing background [16]. New deep multi-wavelength surveys like the Great Observatories Origins Deep Survey (GOODS), described by M.Dickinson, M.Giavalisco and H.Ferguson in this conference, provide significant constraints on the space density of less luminous QSOs at high redshift. Here we present a search for high- z QSOs, identified in the two GOODS fields on the basis of deep imaging in the optical (with *HST*) and X-ray (with *Chandra*), and discuss the allowed space density of QSOs in the early universe, updating the results presented in [6].

2 The Database

The optical data used in this search have been obtained with the ACS onboard HST, as described by M.Giavalisco. Mosaics have been created from the first three epochs of observations, out of a total of five, in the bands $F435W(B_{435})$, $F606W(V_{606})$, $F775W(i_{775})$, $F850LP(z_{850})$. The catalogs used to select high- z QSOs have been generated using the SExtractor software, performing the detection in the z_{850} band and then using the isophotes defined during this process as apertures for photometry in the other bands. This is a common practice avoiding biases due to aperture mismatch coming from independent detections.

The X-ray observations of the HDF-N and CDF-S consist of 2 Ms and 1 Ms exposures, respectively, providing the deepest views of the Universe in the 0.5–8.0 keV band. The X-ray completeness limits over 90% of the area of the GOODS fields are similar, with flux limits (S/N= 5) of 1.7×10^{-16} erg cm $^{-2}$ s $^{-1}$ (0.5–2.0 keV) and 1.2×10^{-15} erg cm $^{-2}$ s $^{-1}$ (2–8 keV) in the HDF-N field, and $\approx 2.2 \times 10^{-16}$ erg cm $^{-2}$ s $^{-1}$ (0.5–2.0 keV) and $\approx 1.5 \times 10^{-15}$ erg cm $^{-2}$ s $^{-1}$ (2–8 keV) in the CDF-S field. The sensitivity at the aim point is about 2 and 4 times better for the CDF-S and HDF-N, respectively. As an example, assuming an X-ray spectral slope of $\Gamma = 2.0$, a source detected with a flux of 1.0×10^{-16} erg cm $^{-2}$ s $^{-1}$ would have both observed and rest-frame luminosities of 8×10^{42} erg s $^{-1}$, and 3×10^{43} erg s $^{-1}$ at $z = 3$, and $z = 5$, respectively (assuming no Galactic absorption). [1] produced point-source catalogs for the HDF-N and CDF-S and [9] for the CDF-S with more than 1000 detected sources in total.

3 The Selection of the QSO candidates

We have carried out the selection of the QSO candidates in the magnitude interval $22.45 < z_{850} < 25.25$. Four optical criteria have been tailored on the basis of typical QSO SEDs in order to select QSOs at progressively higher redshift in the interval $3.5 \lesssim z \lesssim 5.2$. The criteria have been applied independently and produced in total 645 candidates in the CDF-S and 557 in the HDF-N. They select a broad range of high- z AGN, not limited to broad-lined (type-1) QSOs, and are less stringent than those typically used to identify high- z galaxies. We have checked the criteria against QSOs and galaxies known in the literature within the magnitude and redshift ranges of interest confirming the high completeness of the adopted criteria.

Below $z \simeq 3.5$ the typical QSO colors in the ACS bands move close to the locus of stars and low-redshift galaxies. Beyond $z \simeq 5.2$ the $i - z$ color starts increasing and infrared bands would be needed to identify QSOs efficiently with an “ i -dropout” technique.

4 Match with Chandra Sources

The optical candidates have been matched with X-ray sources detected by Chandra within an error radius corresponding to the 3σ X-ray positional uncertainty.

With this tolerance the expected number of false matches is five and indeed two misidentifications, i.e. cases in which a brighter optical source lies closer to the X-ray position, have been rejected (both in the CDF-S).

The sample has been reduced in this way to 11 objects in the CDF-S and 6 in the HDF-N. Type-1 QSOs with $M_{1450} < -21$, given the measured dispersion in their optical-to-X-ray flux ratio [19], are detectable in our X-ray observation up to $z \gtrsim 5.2$. Conversely, any $z > 3.5$ source in the GOODS region detected in the X-rays must harbor an AGN ($L_x(0.5 - 2 \text{ keV}) \gtrsim 10^{43} \text{ erg s}^{-1}$).

5 Redshifts of the QSO candidates

Twelve objects out of the 17 selected have spectroscopic confirmations. Nine are QSOs with redshifts between 2.6 and 5.2. Three are reported to be galaxies, and the relatively large offsets between the X-ray and optical positions suggest that they could be misidentifications. Both quasars of Type I and II are detected.

Photometric redshifts of the 17 QSO candidates have been estimated by comparing with a χ^2 technique (see [2] for details) the observed ACS colors to those expected on the basis of *a*) the typical QSO SEDs; *b*) a library of template SEDs of galaxies (the “extended Coleman” of [2]). For the nine QSOs with spectroscopic confirmation the photometric redshifts are in good agreement with the observed ones. In general the estimates *a*) and *b*) are similar, since the color selection criteria both for galaxies and QSOs rely on a strong flux decrement in the blue part of the spectrum - due to the IGM and possibly an intrinsic Lyman limit absorption - superimposed on an otherwise blue continuum. If we limit ourselves to the redshift range $z > 4$ - where the selection criteria and the photometric redshifts are expected to be most complete and reliable - in addition to one spectroscopically confirmed QSO (HDF-N 123647.9+620941, $z = 5.186$) we estimate that between 1-2 more QSOs are present in the GOODS, depending on whether galaxy or QSO SEDs are adopted for the photometric redshifts. This brings the total to no more than three QSOs with redshift larger than 4.

6 Comparison with the models

Let us compare now the QSO counts observed in the z_{850} band with two phenomenological and two more physically motivated models. The double power-law fit of the 2QZ QSO LF [5] has been extrapolated for $z > 2.7$ (the peak of QSO activity) in a way to produce a power-law decrease of the number of bright QSOs by a factor 3.5 per unit redshift interval, consistent with the $3.0_{-0.9}^{+1.3}$ factor found by [7] for the bright part of the LF. The extrapolation is carried out either as a Pure Luminosity Evolution (PLE) or a Pure Density Evolution (PDE). The PLE model predicts about 17 QSOs with $z_{850} < 25.25$ at redshift $z > 4$ (27 at $z > 3.5$) in the 320 arcmin^2 of the two GOODS fields, and is inconsistent with the observations at a more than 3σ level. The PDE estimate is 2.9 QSOs at $z > 4$ (6.7 at $z > 3.5$).

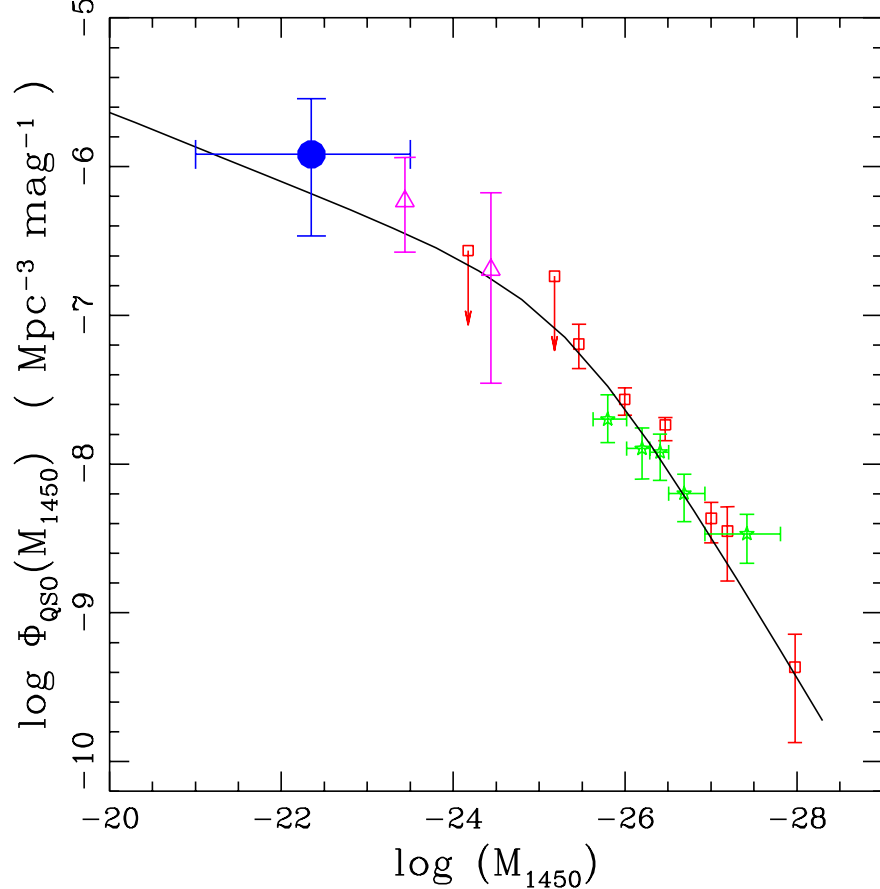


Fig. 1. Differential QSO luminosity function at $z \sim 4 - 5$. Squares: data from [13] and upper limits from [14] at $z \sim 4.4$. Stars: SDSS [7] computed at $3.5 < z < 5$ assuming a power-law decline and rescaled to $z = 4.3$. Triangles: COMBO-17 LF [20], for $4.2 < z < 4.8$. Circle: GOODS LF at $4 < z < 5.2$. The continuous line shows the prediction of the PDE model described in the text. All LFs have been rescaled to a cosmology with $h, \Omega_{\text{tot}}, \Omega_m, \Omega_A = 0.7, 1.0, 0.3, 0.7$.

It is possible to connect QSOs with dark matter halos (DMH) formed in hierarchical cosmologies with a minimal set of assumptions (MIN model, e.g. [11]): *a*) QSOs are hosted in newly formed halos with *b*) a constant SMBH/DMH mass ratio ϵ and *c*) accretion at the Eddington rate. The bolometric LF of QSOs is then expressed by:

$$\Phi(L|z)dL = n_{\text{PS}}(M_H|z) \int_{t(z)-t_{\text{duty}}}^{t(z)} P(t_f|M_H, t(z)) dt_f \epsilon^{-1} \frac{dL}{L_{\text{Edd}}} \quad (1)$$

where the abundance of DMHs of mass M_H is computed using the Press & Schechter [18] recipe, the distribution $P(t_f|M_H, t(z))dt_f$ of the formation times t_f follows [15], t_{duty} is the QSO duty cycle and $L_{Edd} = 10^{4.53} L_\odot$ is the Eddington luminosity of a $1 M_\odot$ SMBH. This model is known to overproduce the number of high- z QSOs [12] and in the present case predicts 151 QSOs at $z > 4$ (189 at $z > 3.5$).

To cure the problems of the MIN model feedback effects have been invoked, for example assuming that the QSOs shine a t_{delay} time after DMH formation (DEL model; [17], [10]). The QSO LF is then computed at a redshift z' corresponding to $t(z) - t_{\text{delay}}$. The predictions of the DEL model are very close to the PDE, with 3.2 QSOs expected at $z > 4$ (4.8 at $z > 3.5$), in agreement with the observations. While all the models presented here are consistent with the recent QSO LF measurement of the COMBO-17 survey [20] at $z \simeq 2 - 3$, only the PDE and DEL models fit the COMBO-17 LF in the range $4.2 < z < 4.8$ and $M_{1450} < -26$.

7 Conclusions

At $z > 4$ the space density of moderate luminosity ($M_{1450} \simeq -23$) QSOs is significantly lower than the prediction of simple recipes matched to the SDSS data, such as a PLE evolution of the LF or a constant universal efficiency in the formation of SMBH in DMH. A flattening of the observed high- z LF is required below the typical luminosity regime ($M_{1450} \lesssim -26.5$) probed by the SDSS. An independent indication that this flattening must occur comes from the statistics of bright lensed QSOs observed in the SDSS [21] that would be much larger if the LF remains steep in the faint end. A similar result has been obtained at $5 \lesssim z \lesssim 6.5$, by [4]. The QSO contribution to the UV background is insufficient to ionize the IGM at these redshifts. This is an indication that at these early epochs the formation or the feeding of SMBH is strongly suppressed in relatively low-mass DMH, as a consequence of feedback from star formation [10] and/or photoionization heating of the gas by the UV background [12], accomplishing a kind of inverse hierarchical scenario.

References

1. Alexander, D.M., et al. 2003, AJ 126, 539
2. Arnouts, S., Cristiani, S., Moscardini, L., Matarrese, S., Lucchin, F., Fontana, A., Giallongo, E., 1999, MNRAS 310, 540
3. Barger, A.J., Cowie, L.L., Richards, E.A., 2000, AJ 119, 2092
4. Barger, A.J., Cowie, L.L., Capak, P., Alexander, D.M., Bauer, F.E., Brandt, W.N., Garmire, G.P., Hornschemeier, A.E., 2003, ApJ 584, L61
5. Boyle, B.J., Shanks, T., Croom, S.M., Smith, R.J., Miller, L., Loaring, N., & Heymans, C., 2000, MNRAS 317, 1014
6. Cristiani, S., et al. 2004, ApJ 600, L119
7. Fan, X., Strauss, M.A., Schneider, D., et al., 2001, AJ 121, 54

8. Fan, X., Strauss, M.A., Schneider, D.P., Becker, R.H., et al., 2003, AJ 125, 1649
9. Giacconi, R., et al. 2002, ApJS 139, 369, G02
10. Granato, G.L., Silva, L., Monaco, P., Panuzzo, P., Salucci, P., De Zotti, G., Danese, L., 2001, MNRAS 324, 757
11. Haiman, Z., & Hui, L., 2001, ApJ 547, 27
12. Haiman, Z., Madau, P., & Loeb, A., 1999, ApJ 514, 535
13. Kennefick, J.D., Djorgovski, S.G., & de Carvalho, 1995, AJ 110, 2553
14. Kennefick, J.D., Djorgovski, S.G., & Meylan, G., 1996, AJ 11, 1816
15. Lacey, C., & Cole, S., 1993, MNRAS 262, 627
16. Madau, P., Haardt, F., Rees, M.J., 1999, ApJ 514, 648
17. Monaco, P., Salucci, P., Danese, L., 2000, MNRAS 311, 279
18. Press, W.H., & Schechter, P., 1974, ApJ 187, 425
19. Vignali, C., et al. 2003, AJ 125, 2876
20. Wolf, C., Wisotzki, L., Borch, A., Dye, S., Kleinheinrich, M., Meisenheimer, K., 2003, A&A 408, 499
21. Wyithe, J.S.B., Loeb, A., 2002, ApJ 577, 57